Polarity-controlled visible/infrared electroluminescence in Si-nanocrystal/Si light-emitting devices

Zhihong Liu,[1] Jiandong Huang,[2,a)] Pooran C. Joshi,[2] Apostolos T. Voutsas,[2] John Hartzell,[2] Federico Capasso,[3] and Jiming Bao[1,b)]
[1]*Department of Electrical and Computer Engineering, University of Houston, Houston, Texas 77204, USA*
[2]*Materials and Devices Applications Laboratories, Sharp Laboratories of America, Camas, Washington 98607, USA*
[3]*School of Engineering and Applied Sciences, Harvard University, Cambridge, Massachusetts 02138, USA*

(Received 5 December 2009; accepted 1 July 2010; published online 18 August 2010)

We report the demonstration of a room-temperature visible/infrared color-switchable light-emitting device comprising a Si nanocrystal-embedded silicon oxide thin film on a p-type Si substrate. The device emits band-edge infrared light from the silicon substrate when the substrate is positively (forward) biased with respect to the Si-nanocrystal film. Under reverse bias, visible emission from the Si-nanocrystal film is observed. Compared to the photoluminescence of the Si-nanocrystal film, the visible electroluminescence is broader and blueshifted to shorter wavelength, and is ascribed to impact ionization in the Si-nanocrystal/SiO_2 film. © *2010 American Institute of Physics*. [doi:10.1063/1.3480403]

Silicon (Si) photonics has attracted much attention for the past several decades.[1,2] One of its goals is to develop Si-based light-emitting devices that are compatible with Si microelectronic technology. Si nanocrystals (Si-ncs) have shown enhanced light emission at visible and near infrared wavelengths due to the quantum confinement effect.[1,2] Enhanced band-edge emission has also been observed in Si metal-insulator-semiconductor (MIS) structures.[3,4] Here, we report the demonstration of color-switchable Si-nc LEDs that take advantage of visible emission from silicon nanocrystals and infrared from the Si substrate.[5,6] We show that the emission bands of devices can be controlled by the polarity of applied bias voltage: infrared under forward bias, and visible under reverse bias.

The LEDs consist of a 50-nm-thick layer of Si-nc oxide thin film deposited on top of a p^+-silicon substrate (~0.02 Ω cm). The thin film was grown using high-density plasma enhanced chemical vapor deposition with a SiH_4 to N_2O ratio of 1.33, and the film was subsequently annealed at 1000 °C for 30 min to ensure nucleation of Si-nc from the SiO_2 matrix. Using a sputtering tool, indium tin oxide (ITO) was subsequently deposited on top of Si-nc thin films to serve as transparent electrical contact. The top ITO contact was patterned using standard photolithography. Room-temperature photoluminescence (PL) and electroluminescence (EL) measurements were performed using a spectrometer equipped with a Si charge-coupled device (CCD) for visible light detection and an InGaAs array detector for infrared light detection.

The PL spectrum (PL-Si-nc) of the Si-nc film is shown in Fig. 1(a); it exhibits a broad emission centered at 850 nm. To obtain this spectrum, we measured PL (PL-Si-nc/Si) from the LED surface as well as PL (PL-Si) from the same bare Si substrate used for the LED, as shown in the insets of Fig. 1(a). We have also compared PL spectra from surface regions either covered with or clear of ITO contacts. No detectable difference in the PL spectrum was observed, indicating that

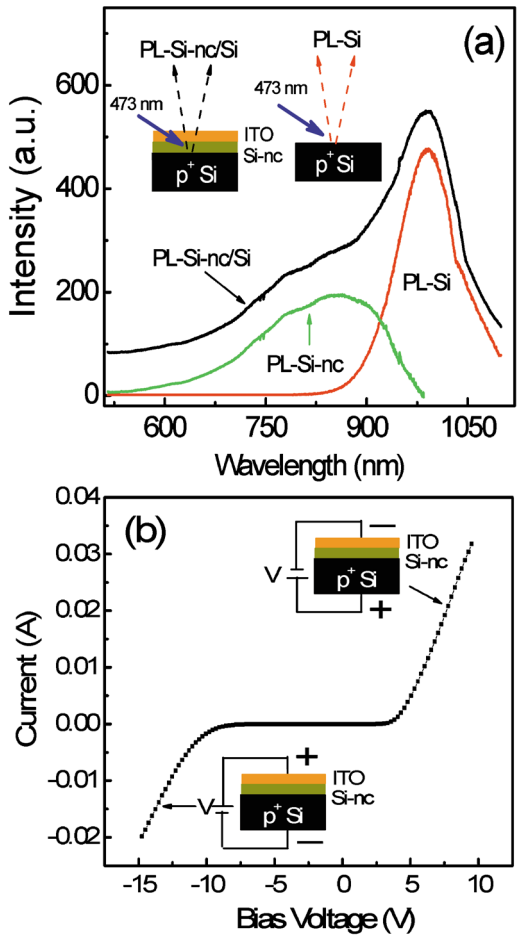

FIG. 1. (Color online) (a) PL spectra measured with the Si CCD. (PL-Si-nc/Si) PL emitted from the LED surface (inset on the left). Because both the Si-nc thin film and the Si substrate are excited by the λ=473 nm laser, they both contribute to the PL. (PL-Si) PL from the bare Si substrate (inset at the center) used for the LED; here the PL spectrum is scaled so that it has the same peak intensity at 1100 nm as the Si-nc/Si PL. (PL-Si-nc) Si-nc PL is obtained after subtracting the Si PL in red from Si-nc/Si PL in black. The Si-nc/Si PL spectrum is shifted vertically for clarity. The drop in intensity at wavelengths longer than 1000 nm is due to the cutoff response of the Si CCD. (b) Current-voltage characteristics of the Si-nc/Si LED. Forward bias corresponds to a positive voltage on the p-type substrate as shown in the inset.

a)Electronic mail: jhuang@sharplabs.com.
b)Electronic mail: jbao@uh.edu.

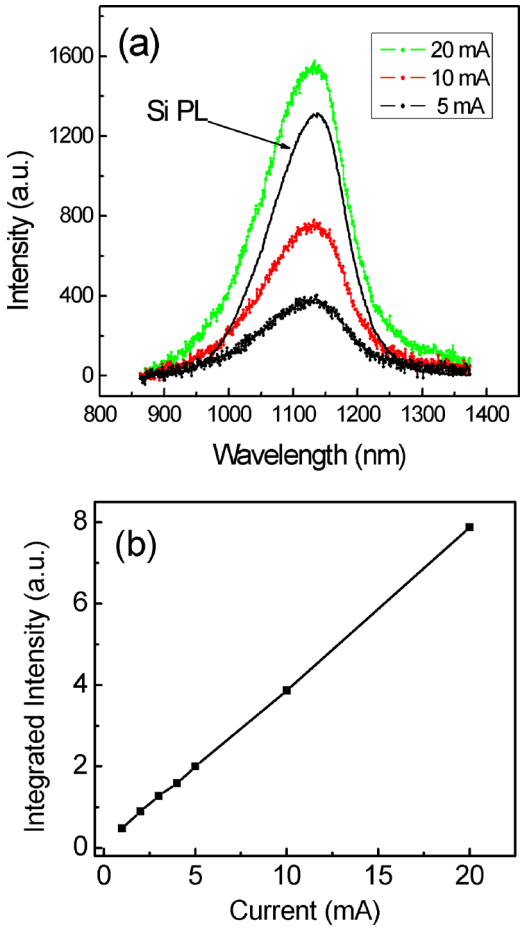

FIG. 2. (Color online) (a) Forward-bias EL spectra at currents of 5, 10, and 20 mA. The solid black curve is PL of the Si substrate. The EL and PL spectra are measured using the InGaAs detector. (b) Integrated EL intensity as a function of current.

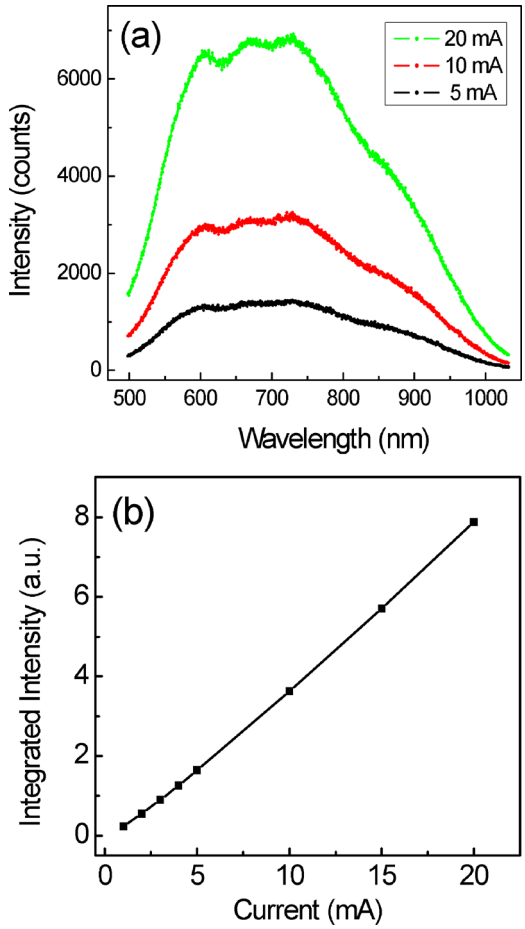

FIG. 3. (Color online) (a) EL of the LED under reverse bias at currents of 5, 10, and 20 mA. The spectra are obtained using the Si CCD. (b) Integrated EL intensity as a function of current.

no measurable PL can be attributed to the ITO layer. The current-voltage (I-V) curve of the device, shown in Fig. 1(b), exhibits a good rectifying behavior. The current starts to increase rapidly when forward bias is greater than ~4 V. In contrast, the reverse current does not turn on until the reverse bias voltage exceeds ~8.5 V.

Infrared emission is observed when the device is forward biased, and representative spectra at three different currents are shown in Fig. 2(a). The three EL spectra are very similar in shape, resembling the Si PL spectrum [Fig. 2(a)]. All of these spectra were measured using the InGaAs array detector. In addition, the Si CCD was also used to detect any visible emission, and no measurable EL similar to the PL of Si-nc was observed. The integrated emission intensity as a function of input current is shown in Fig. 2(b), and a nearly linear dependence is observed within the measured current range.

The infrared emission centered at 1130 nm disappears when the LED is reverse biased, but a broadband visible luminescence is observed using the Si CCD. As can be seen in Fig. 3(a), spectra at different currents are also very similar in shape, with a stronger intensity in the 600–800 nm spectral range. Compared with the PL of the Si-nc, the EL is broader and blueshifted to shorter wavelengths. The integrated emission intensity is also nearly linearly dependent on current, as shown in Fig. 3(b).

Si band-edge infrared emission and visible EL have been observed in different MIS structures[3–9] and Si-nanocrystal LEDs.[10–12] In general, emission spectra and the associated microscopic origins strongly depend on the material, device configuration, and operating condition. In order to understand the electrical and optical properties of the device, we calculate the distribution of bias voltage across the LED.[5,7,13–15] Figure 4 shows the band diagrams of the LED at a negligible current (10 μA) under forward and reverse biases. Here, we approximate the Si-nc/SiO_2 matrix as a uniform SiO_2 thin film with a dielectric constant of ~5 measured by ellipsometry. This approximation is valid because of the thickness of Si-nc/SiO_2 film (50 nm) compared with the size of Si nanocrystals. The uniformity of the film is also confirmed by the uniform infrared and visible EL across a large area of the film.

The band diagrams reveal important features that can qualitatively explain the rectifying characteristics and EL properties of the LED. As can be seen from Fig. 4, the majority of external bias voltage is dropped across the Si-nc/SiO_2 film. The band bending in Si near the interface is negligibly small compared with the total bias voltage, especially in the case of forward bias. This picture remains the same at a higher bias voltage. The rectifying behavior of the LED arises from the heavy p-doping and the consequent different space charge at the interface. Under forward bias, an accumulation layer of holes is formed, and electrons tunnel from ITO to the Si substrate through Si-nc/SiO_2 film. However, the accumulation layer becomes depleted under reverse bias, and the tunneling current of electrons from Si to ITO

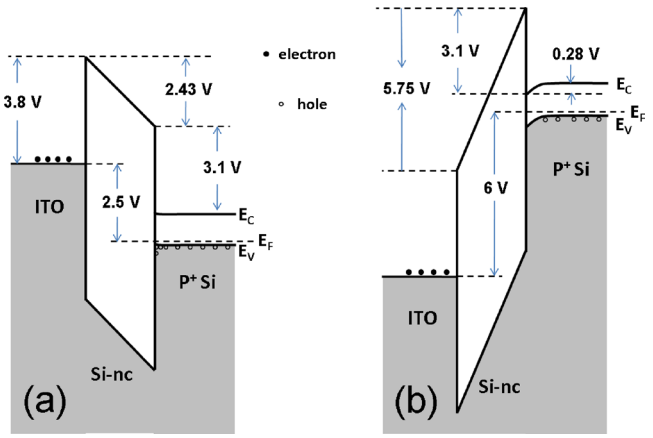

FIG. 4. (Color online) Schematic band diagrams of the device under forward bias (a) and reverse bias (b) at a small current of ~10 μA. The 6 V reverse bias and the 2.5 V forward bias voltages are deduced from the I-V curve in Fig. 1(b). The work function of ITO (4.7 eV) and band offsets between SiO_2 and Si are taken from Refs. 5, 7, and 13–15. Note that at the reverse bias of 6 V the interface between the Si-nc thin film and the Si substrate is depleted of electrons. As shown in Fig. 1(b) a larger reverse bias voltage is needed to induce EL, because as explained in the text the latter originates from electrons tunneling from the inversion layer at the thin film-substrate interface.

will remain small until an inversion layer of electrons is formed at the interface with P^+ Si. The calculation shows that the threshold for the creation of an inversion layer is ~8.3 V, which agrees well with the observed onset voltage for large current in reverse bias as shown in Fig. 1(b). In contrast, the forward current does not increase drastically until field-enhanced Fowler–Nordheim tunneling takes effect,[1,2,11]—i.e., when the voltage drop across the Si-nc/SiO_2 layer equals the band offset between ITO and the film. The required turn-on voltage of ~3.8 V can also be clearly seen from the I-V curve in Fig. 1(b).

In the above discussions, we have neglected the tunneling current of holes, which is much smaller than that of electrons for the following two reasons:[1,2,5,7,11,13] (1) holes experience a higher potential barrier because of a large valence band offset at interfaces between SiO_2 and ITO, and between SiO_2 and Si (Fig. 4); (2) holes have a larger effective mass and a lower mobility. These differences between electrons and holes are the key to understanding the observed device behavior.

It is relatively straightforward to assign the infrared EL in the forward bias to the Si band-edge luminescence due to the good agreement between the EL with the PL of Si as shown in Fig. 2(a). The band-edge EL is a result of radiative recombination of holes confined at the interface with electrons that tunnel from ITO to the Si substrate through the Si-nc/SiO_2 film. However, the origin of visible EL in reverse bias in similar MIS structures has been controversial. It was proposed that this visible emission comes from impact ionization of hot electrons in the Si substrate.[10] We can rule out this possibility in our case. As discussed above, the band bending of Si near the interface is on the order of ~1 V even at a large reverse bias voltage, so the energy gained by electrons is not large enough to create electron-hole pairs with a broadband emission.

We can conclude that under reverse bias the visible EL originates from Si-nc/SiO_2 matrix, and that the impact ionization is the most probable mechanism for the broadband EL, by which accelerated high-energy electrons originating in the inversion layer create electron-hole pairs in Si-nanocrystals.[7,11] This visible EL is certainly not due to injection of electrons and holes into Si-nc film because a direct injection of holes into Si-nc film from ITO is very weak. Furthermore, the I-V curve shows characteristics of a unipolar injection as discussed above. The same reasons can explain the absence of visible EL under forward bias. In fact, injection of electrons and holes into Si-nc has been challenging even at a forward bias.[11] The low turn-on voltage in forward bias has prevented us from obtaining a strong enough electrical field for impact ionization, as occurred in reverse bias. The reason that a super-linear dependence of EL on current was not observed is probably due to other competing nonradiative processes, such as Auger recombination at a higher injection.[11]

MIS silicon infrared devices usually require a thin and high-quality oxide layer that is difficult to control during growth.[5] By replacing the demanding high-barrier oxide layer with Si-nc/SiO_2 thin films of low effective barrier in our devices, we can increase the thickness of this insulating layer up to ~100 nm compared with 2–3 nm of silicon oxide without sacrificing the low turn-on voltages. A uniform emission is observed over the whole ITO layer of the devices, in contrast to ITO layer with pinholes observed in some MIS devices. A thick, uniform Si-nc film can dramatically enhance the device stability and lifetime.

In conclusion, we have demonstrated polarity-switchable, visible/infrared Si-nc devices. Band-edge infrared emission originates from electron and hole radiative recombination in Si at the interface of the Si-nc/SiO_2 film and the silicon substrate under forward bias, while visible emission originates from the Si-nc thin film due to impact ionization under reverse bias. The devices could find applications in large-area displays.

J. M. Bao acknowledges supports from Texas Center for Superconductivity at the University of Houston.

[1] D. J. Lockwood and L. Pavesi, *Silicon Photonics* (Springer, New York, 2004).
[2] S. Ossicini, L. Pavesi, and F. Priolo, *Light Emitting Si for Microphotonics, Springer Tracts in Modern Physics* (Springer, Berlin, 2003), Vol. 194.
[3] C. W. Liu, M. H. Lee, M.-J. Chen, I. C. Lin, and C.-F. Lin, Appl. Phys. Lett. **76**, 1516 (2000).
[4] T. C. Chen, W. Z. Lai, C. Y. Liang, M. J. Chen, L. S. Lee, and C. W. Liu, J. Appl. Phys. **95**, 6486 (2004).
[5] S. Kuai and A. Meldrum, Physica E (Amsterdam) **41**, 916 (2009).
[6] M. A. Zimmler, J. Bao, I. Shalish, W. Yi, V. Narayanamurti, and F. Capasso, Nanotechnology **18**, 395201 (2007).
[7] D. J. DiMaria, J. R. Kirtley, E. J. Pakulis, D. W. Dong, T. S. Kuan, F. L. Pesavento, T. N. Theis, J. A. Cutro, and S. D. Brorson, J. Appl. Phys. **56**, 401 (1984).
[8] G. F. Bai, Y. Q. Wang, Z. C. Ma, W. H. Zong, and G. G. Qin, J. Phys.: Condens. Matter **10**, L717 (1998).
[9] J. Yuan and D. Haneman, J. Appl. Phys. **86**, 2358 (1999).
[10] S. Fujita and N. Sugiyama, Appl. Phys. Lett. **74**, 308 (1999).
[11] A. Marconi, A. Anopchenko, M. Wang, G. Pucker, P. Bellutti, and L. Pavesi, Appl. Phys. Lett. **94**, 221110 (2009).
[12] R. J. Walters, G. I. Bourianoff, and H. A. Atwater, Nat. Mater. **4**, 143 (2005).
[13] S. M. Sze, *Physics of Semiconductor Devices*, 2nd ed. (Wiley, New York, 1981).
[14] E. Centurioni and D. Iencinella, IEEE Electron Device Lett. **24**, 177 (2003).
[15] B. Averboukh, R. Huber, K. W. Cheah, Y. R. Shen, G. G. Qin, Z. C. Ma, and W. H. Zong, J. Appl. Phys. **92**, 3564 (2002).